

High-intensity ribbons in multiply scattering media

B. J. USCINSKI^{†‡} and M. SPIVACK^{*†}

[†]Department of Applied Mathematics and Theoretical Physics, Centre for Mathematical Sciences,
University of Cambridge, Wilberforce Road, Cambridge, UK

[‡]Applied Physics Laboratory, University of Washington, 1013 NE 40th Street, Seattle,
WA 98105-6698, USA

The origins of the long, high-intensity ribbons that occur when a wave propagates through a multiply scattering random medium are examined. It is shown that such ribbons are initiated when the cumulative phase deviation imposed on the wavefront in the direction of propagation becomes large. Estimates are made of the number of such ribbons that might be encountered in typical cases of multiple scatter, and of their expected separation transverse to the direction of propagation. Finally, it is shown that motion of the source in the transverse direction does not lead to appreciable movement of the ribbons.

1. Introduction

When a sound or light wave propagates through a medium with random inhomogeneities of refractive index, intensity fluctuations arise [1–4]. These can be large in the case of multiple scattering and have been much studied both theoretically [5] and experimentally [6]. A striking feature in the spatial structure of the fluctuating field is the presence of long ribbons of quite high intensity. They can extend for very many irregularity correlation lengths in the direction of wave propagation. These high-intensity ribbons have been observed and studied in numerical simulations of wave propagation in random media, and have also been detected experimentally in the case of sound propagation in the ocean. Existing theoretical studies of intensity fluctuations deal principally with ensemble averaged quantities such as mean intensity or variance and (usually transverse) correlation functions (e.g. [7, 8]); these studies yield little information about the ribbons and their typical spatial structure, which appear in individual realizations of the medium and are effectively smoothed out by ensemble averages. On the other hand, both high- and low-intensity regions are found to remain remarkably stable under changes in the source position or angle. This is an issue of considerable practical importance in certain applications, including underwater sonar detection and navigation.

This paper addresses some key questions about the ribbons that remain unanswered. One of these is their origin, and the extent to which they arise from specific identifiable features of the scattering medium. The answers offer insight into why, once started, they persist for so many scattering lengths in the medium. The second aspect that is considered is the number and separation of the ribbons. Often only a single ribbon is encountered over several irregularity correlation lengths transverse to the direction of propagation. The question arises as to what

*Corresponding author. E-mail: m.spivack@damtp.cam.ac.uk

dictates the ribbon separation and what is its expectation value, and in particular whether it can be predicted where the ribbons might occur.

In addition we examine how the ribbons behave as the source position is altered, and the extent to which the wavefield structure depends upon this. This is done, first, by averaging numerically over source location, for a given realization. In practice, however, it is the *motion* of the pattern rather than its average which is of interest, and such patterns are presented in accompanying simulations for both a moving source and changing source angle [9, 10].

2. Numerical simulations

Although the literature contains many examples of the numerical simulation of wave propagation in multiply scattering random media, it is convenient to present a further set in order to facilitate discussion of the topics mentioned in the introduction. We shall confine this study to the two-dimensional case with the statistically stationary random medium situated in the positive half plane $x \geq 0$ of a Cartesian set of coordinates (x, z) (figure 1). Denoting the wavespeed of the medium by $c(x, z)$ and its average or reference value by c_0 , the refractive index $r(x, z)$ is then the ratio c_0/c , which has a mean value of unity. It is convenient to write this as $r = 1 + n(x, z)$ (e.g. [2, 11]), so that $n(x, z)$ represents spatial inhomogeneities, i.e. the departure of the refractive index from the mean. These inhomogeneities are assumed to be weak, with magnitude

$$n(x, z) \ll 1 \quad (1)$$

with mean value of zero and variance denoted by μ^2 .

In these examples we assume that the refractive index irregularities are isotropic, with scale size L much larger than the wavelength of the propagating field. The angles of scatter will thus be very small and the parabolic form of the wave equation can be used to describe the

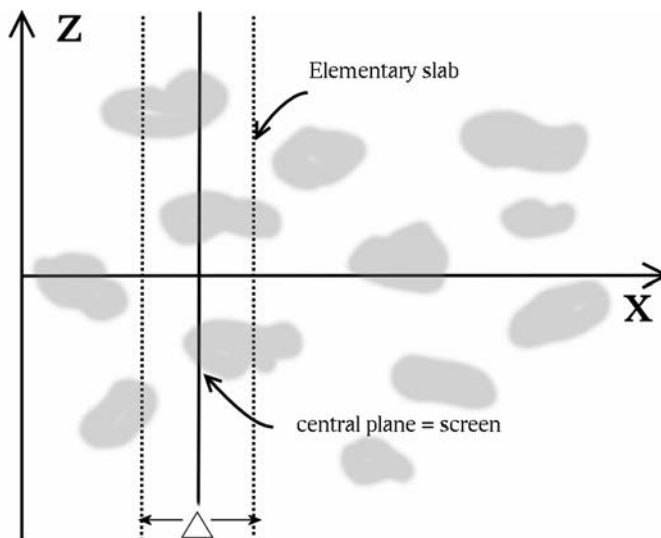


Figure 1. The weakly random medium showing an elementary slab and the central screen onto which the phase of the slab is projected.

behaviour of the complex wave field $A(x, z)$,

$$\frac{\partial A}{\partial x} = -\frac{i}{2k} \frac{\partial^2 A}{\partial z^2} - ik\mu n_1(x, z)A \quad (2)$$

where

$$\mu n_1(x, z) = n(x, z) \quad (3)$$

and k is the wavenumber of the field. The spatial autocorrelation function of the inhomogeneities (e.g. [7, 11]) is

$$\rho(\xi, \zeta) = \langle n_1(x, z)n_1(x + \xi, z + \zeta) \rangle \quad (4)$$

where the angled brackets denote an ensemble average. Various numerical procedures for simulating propagation of the complex field $A(x, z)$ in a weakly irregular medium using the parabolic form of the wave equation (2) are available [12–14]. Typically these methods involve dividing the medium into a set of slabs transverse to the direction of propagation. Each slab, say $[x_n, x_n + \Delta]$, has a thickness Δ that is of the order of one or two correlation lengths L and on passing through it the wavefront acquires a phase modulation $\phi(z)$ given by

$$\phi(z) = k\mu \int_{x_n}^{x_n + \Delta} n_1(x', z) dx' \quad (5)$$

For the simulations the structure in each slab is projected onto a plane situated at the centre of the slab. The medium then consists of a set of phase-changing screens with the phase given by equation (5) whose autocorrelation function is

$$R(\zeta) = k^2 \mu^2 \int \rho(\xi, \zeta) d\xi \quad (6)$$

The well-known split-step algorithm is used [13–15] in which the field $A(x, z)$ passes through a screen which modulates its phase in coordinate space, then its Fourier transform is taken and it is propagated to the next screen in Fourier space. Here it is transformed back into coordinate space and the process is repeated for each screen. Details of this method are given in Appendix A.

In the present example we use the Gaussian representation of a point source, which on the incidence plane $x = 0$ takes the form

$$A(0, z) = A_0 \exp(-[z - z_0]^2/w^2) \quad (7)$$

centred on $(0, z_0)$ and with a width w that can be varied as desired. More generally for a directed beam at some small angle θ to the horizontal this acquires a phase factor $\exp(ikS[z - z_0]/2)$. In an undisturbed medium in the absence of irregularities, at a distance x from the plane of incidence this would take the form

$$A(x, z) = \frac{w}{\sqrt{w^2 + 2ix/k}} \exp\left[-\frac{2z^2 + ikSw^2(Sx - z)}{2(w^2 + 2ix/k)}\right] \quad (8)$$

For simplicity we have chosen the medium autocorrelation function

$$\rho(\xi, \zeta) = \exp(-[\xi^2 + \zeta^2]/L^2) \quad (9)$$

which leads to

$$R(\zeta) = \sqrt{\pi} k^2 \mu^2 L \exp(-\zeta^2/L^2) \quad (10)$$

We then introduce the scaled coordinates

$$Z = z/L, \quad X = x/kL \quad (11)$$

We now present some results of propagation in the above medium. In the following simulation, the intensity values at each range x have been rescaled so that the maximum value at that range is unity. This is done in order to depict the ribbon structure more clearly. The first simulation [figure 2(a)] shows the high-intensity ribbons for the source at $z = 0$, as a colour contour plot. The ribbons extend through very many screens, i.e. many correlation lengths in the direction of

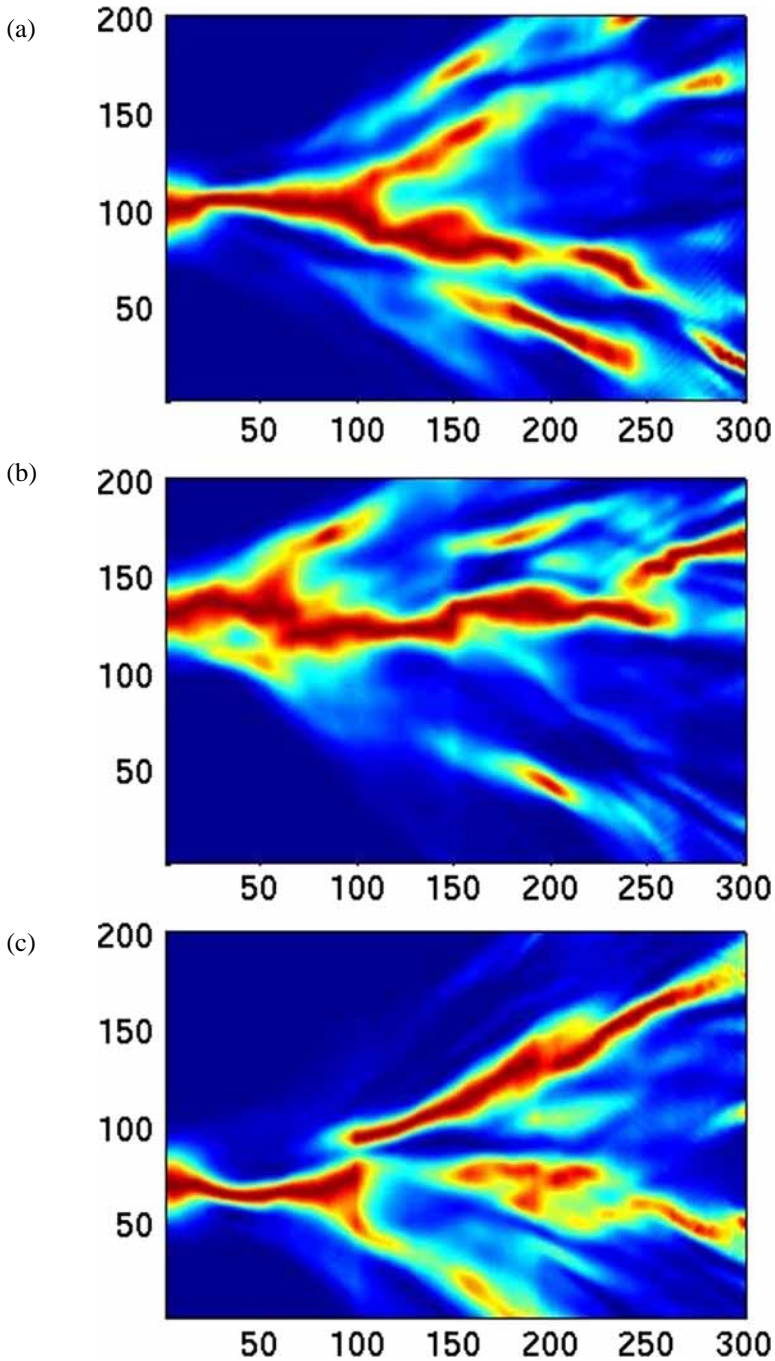


Figure 2. Ribbons with source at (a) $(0, 0)$, (b) $(0, a)$, and (c) $(0, -a)$.

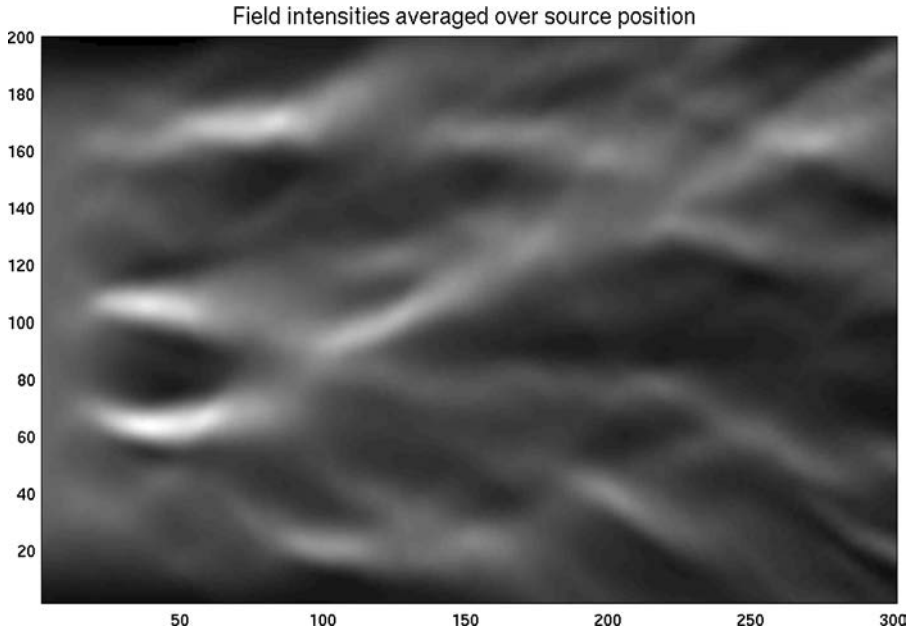


Figure 3. Intensity pattern averaged over vertical distribution of source position.

propagation. In the transverse (vertical) direction the solution domain extends to 40 correlation lengths, of which the central region of around ten correlation lengths is shown.

The source is then moved to $z = +a$ [figure 2(b)] and $z = -a$ [figure 2(c)], where

$$a \cong 1.5L \quad (12)$$

The main structure of the ribbons remains broadly the same as the source position changes. It is also apparent that some regions are not substantially insonified, and these ‘quiet regions’ also stay largely unchanged. To a large extent these intensity patterns are therefore attached to features in the medium and, in effect, moving the source just illuminates a different part of the medium. This becomes clearer by taking an average of the intensity pattern with respect to source location: this is shown in figure 3, which results from varying the source position and integrating in equal steps vertically along the z axis. In practical applications, of course, it is more often the moving source rather than the average which is of interest (and in fact the observer will very effectively detect by eye persistent features in moving patterns). The characteristic changing intensity pattern as the source position is moved continuously, and as the beam angle is varied, can be seen respectively in [9] and [10]. Several regions in both the near and far field of the incidence plane are never significantly insonified. Note that in ocean acoustics the time-scale over which the medium changes significantly may be slow relative to the movement of, for example, a submarine-based sonar. We now need to consider in more detail the irregular medium that produces the ribbons, before further theoretical consideration in section 4 and Appendix C.

3. The irregular medium

The extended random scattering medium has been converted to a set of weak phase-changing screens, as described above. We can investigate the relationship between the scattering medium

and the high intensity ribbons by adding the phase modulations produced by successive screens in the direction of propagation. Thus, the cumulative phase modulation imposed by the medium on a propagating wavefront is

$$f(x, z) = \sum_i \phi_i, \quad (13)$$

where

$$\phi_i = \phi(x'_i, z) \quad (14)$$

is the phase change introduced by the screen at distance x' . The cumulative modulation for the example given above is shown in figure 4. A tendency can be seen for high-intensity ribbons to develop at places where a large cumulative phase modulation occurs. (This is most marked in the near field, as can be seen by comparison with figure 3). Once started the ribbon tends to persist even though the field subsequently propagates through further regions of the scattering medium, which might naively be expected to destroy the high intensity. The ribbons can be linked to specific features in the medium, thus explaining why they tend to remain in much the same place when the position of the source changes. A further example is given in figures 5–8, for a different realization. Figures 5 and 6 respectively show the intensity averaged over source position and the cumulative phase of the medium itself, and the correlation is again evident. This point is further emphasized by taking the correlation between the two quantities, shown in figure 7. By comparison, the correlation with the medium itself is much weaker, as shown in figure 8. This connection, between medium and ribbon structure, is explored theoretically in the next section and in Appendix 3. It is shown that it is possible to give a slightly more quantitative theoretical treatment of the ribbons to explain the observed connection with the medium.

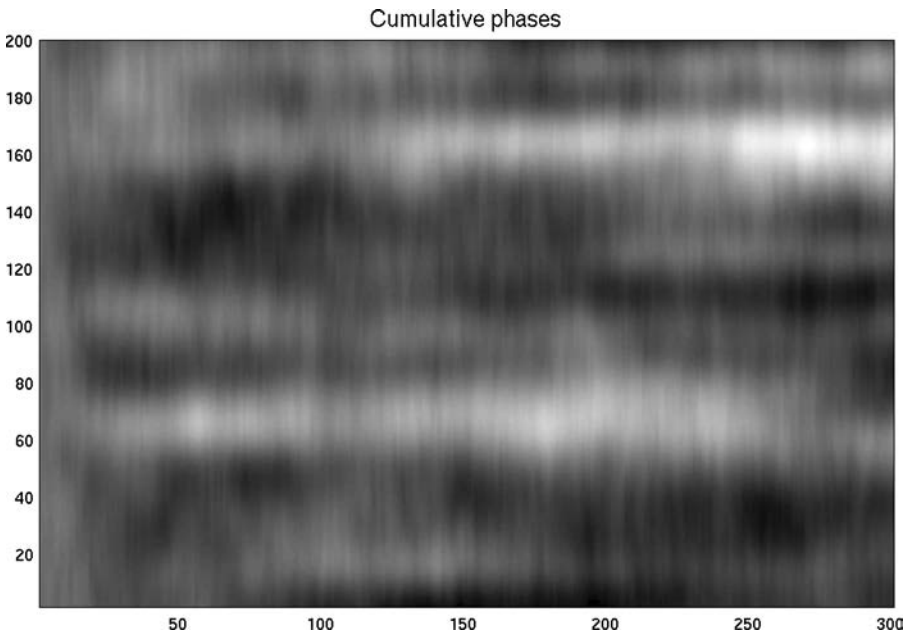


Figure 4. The integrated phase modulation imposed by the medium in the above example at different distances of propagation.

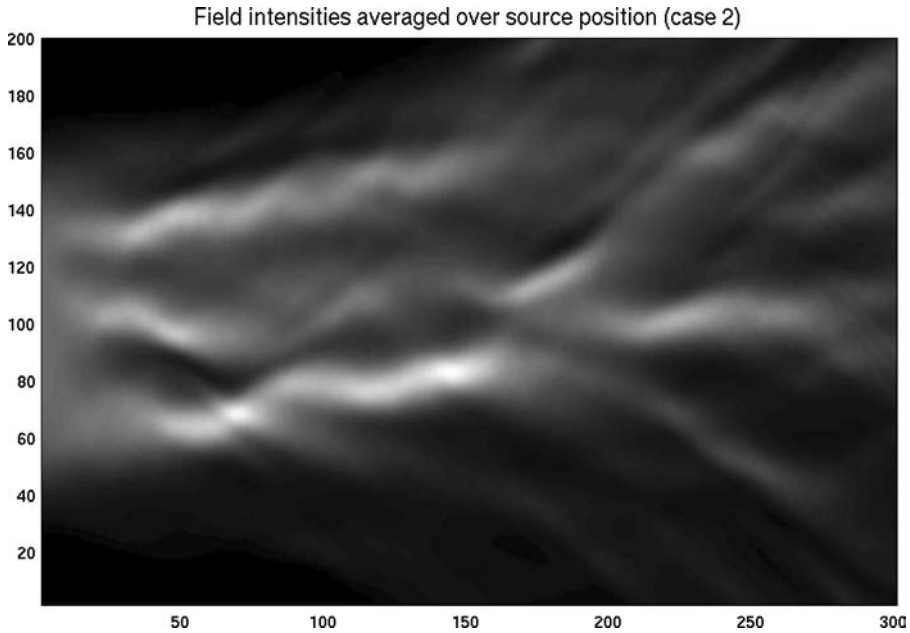


Figure 5. Intensity pattern averaged over vertical distribution of source position (second realization).

4. Wavefront and diffraction

Initially the field from the point source is diverging so that its intensity decreases with distance of propagation. However, as the wavefront passes through the scattering medium it acquires a phase modulation from each slab (screen) that it traverses. The transverse scale size of this

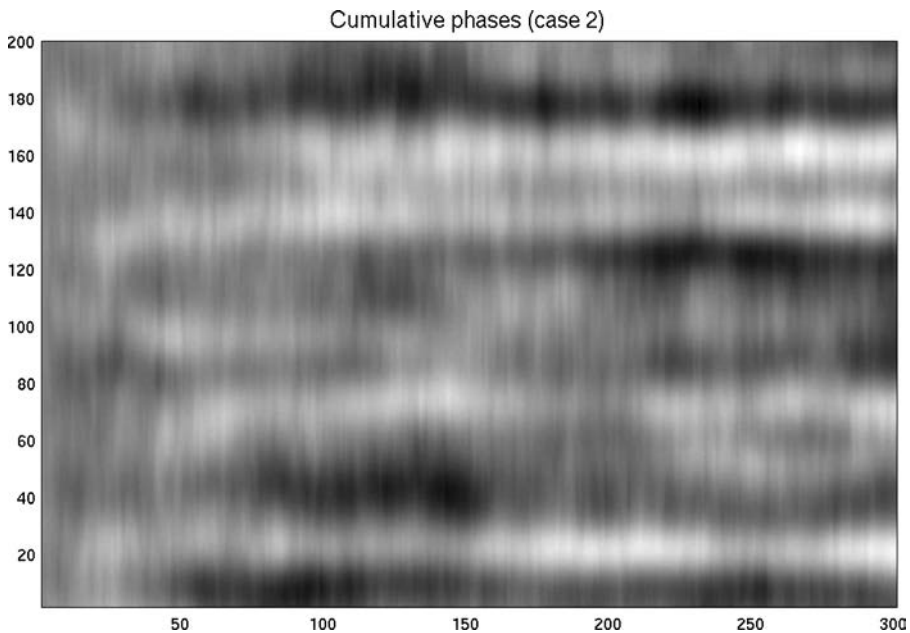


Figure 6. The integrated phase modulation imposed by the medium in the above example at different distances of propagation (second realization).

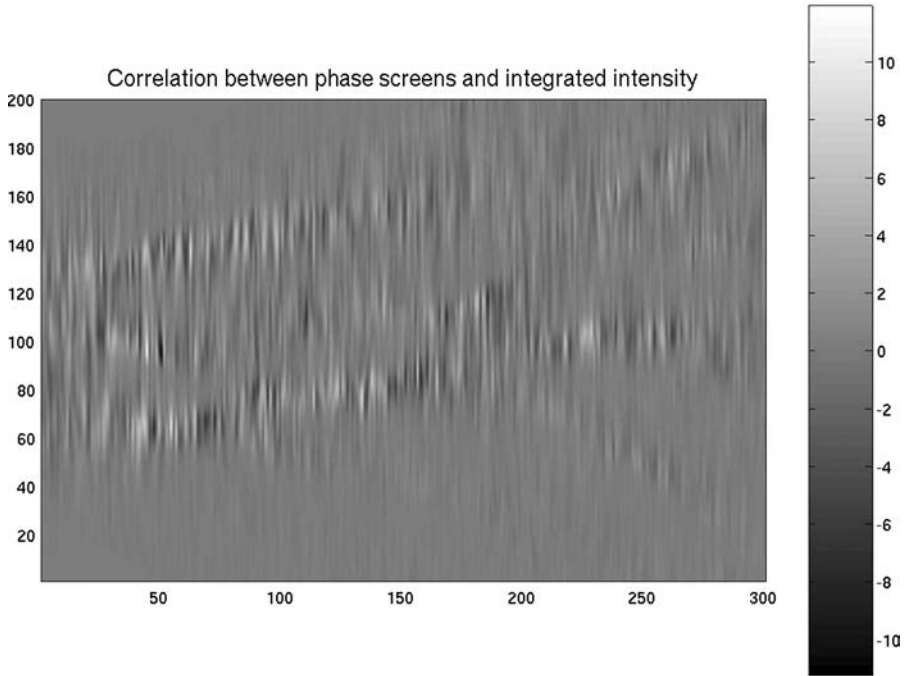


Figure 7. Correlation of cumulative phase and intensity pattern averaged over source position.

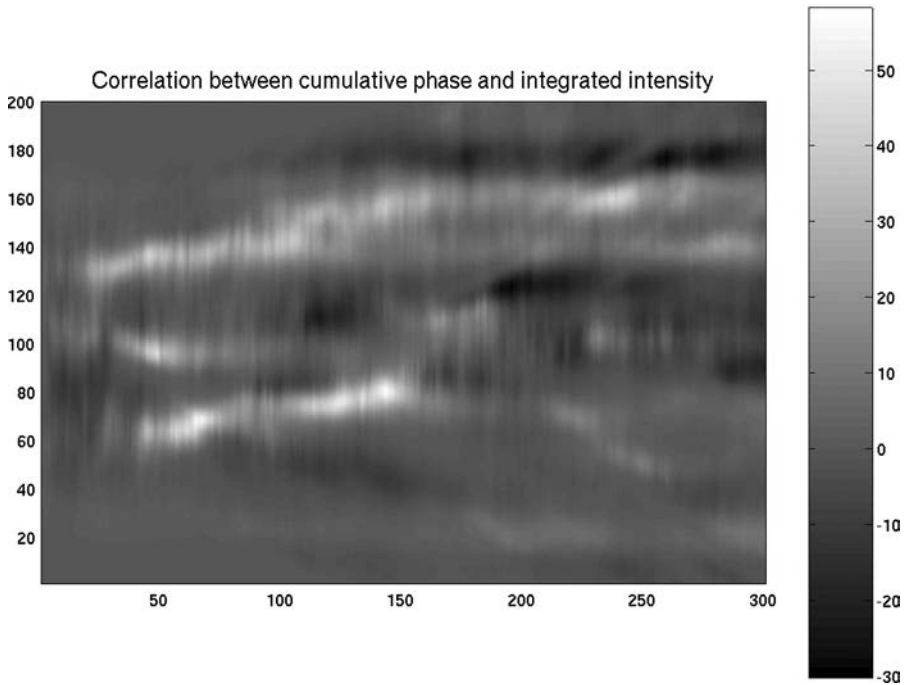


Figure 8. Correlation of phase itself with intensity averaged over source position.

modulation is L , the same as that of the irregular structures in the elementary slab. Simple diffraction considerations show that the focusing phase curvature introduced by features in the screen must be larger than the defocusing phase curvature of the diverging wavefront from the point source for an increase in intensity to occur. If the equivalent phase screens are weak, then the phase modulation will be insufficient for amplification to occur as the wavefront starts to propagate through the medium. However, as each successive screen is traversed, the imposed phase modulation builds up until the wavefront has a large phase curvature and focusing can occur. Appendix B illustrates these points by treating scattering from a single irregularity. It can be seen that the focusing distance [equation (B13)] from the strongly modulated wavefront is

$$kD^2/8f \quad (15)$$

Here f [equation (13)] is the phase modulation imposed on the wavefront which is, in fact, the cumulative phase modulation of all the screens traversed in the medium. Since these are statistically independent their phase contributions add incoherently. The wavefront phase is then a Gaussian random process with scale size L and variance equal to the summed variances of the individual screens. The single screens are weak but their summed variance can be large. The wavefront is now equivalent to a deeply modulated phase screen and it will contain a certain number of regions where the phase excursion and phase curvature (second derivative) are large. Proof that the two tend to occur simultaneously is shown in Appendix C. These regions can lead to strong focusing and large amplitudes.

This then is the origin of the high-intensity ribbons. Although the phase changes from the individual screens are small, and will mostly tend to cancel as a resource of incoherent addition, the variance will grow and there will be cases in which the additions reinforce to produce the big phase excursions. The number of these can be estimated using the fact that the phase excursion of the wavefront follows a normal distribution. If we define large positive phase excursions as those lying above one standard deviation, then we find that only about 8% of the wavefront will fall into this class. For this reason we expect that one high-intensity ribbon will, on average, occur for every ten transverse scale sizes L in the medium. This is admittedly a fairly crude estimate, but it agrees reasonably well with simulations.

The final question remains as to why, once started, a high-intensity ribbon continues for a long way approximately in the direction of propagation. This can be answered by considering the angle of scattering of the field. Even though multiple scattering has occurred the root-mean-square (rms) scattering angle

$$2f/kL \quad (16)$$

is still very small, and it is this scattering angle that dictates the rate of change of amplitude features. This point is also touched on in Appendix D.

5. Conclusions

The high-intensity ribbons that appear when a wave propagates in an extended random medium have been shown to be linked to specific features in the medium itself. They occur where the integrated phase modulation of the wavefront builds up regions that are equivalent to a strongly focusing lens. Straightforward statistical considerations show that the separation of such ribbons transverse to the direction of propagation is of the order of ten scale sizes. The ribbons are expected to be most prominent at the so-called ‘focusing’ region.

It has also been shown that moving the source by even a few scale lengths L does not cause the ribbons to move as a whole. At the most, some details of the ribbon structure change, while some regions remain ‘quiet’ for all source positions.

Appendix A: Formulation and accuracy of the numerical simulations

We summarize here the formulation and accuracy of the numerical method used above. For convenience write equation (2) in operator notation as

$$\frac{\partial A}{\partial x} = (D + G)A \quad (\text{A1})$$

where D is the differential operator $-(i/2k)\partial^2/\partial z^2$ and G is multiplication by $-ik\mu n_1(x, z)$. Then formally the solution of equation (A1) over a small step ξ can be written

$$A(x + \xi, \cdot) \cong \exp \left[\int_x^{x+\xi} (D + G) dx' \right] (A(\xi, \cdot)). \quad (\text{A2})$$

This approximation is accurate to second order in ξ , with a step-wise error of the form $\xi^3[D + G, \partial D/\partial \xi]$ (e.g. 15) where $[\cdot, \cdot]$ denotes the commutator. It is therefore exact if the range-dependent operator $(D + G)$ commutes with its integral, and for G varying moderately in x this approximation is highly accurate.

This suggests the use of the well-known split-step algorithm which was introduced to underwater acoustics by Tappert and Hardin [13] and remains in widespread use. In order to maintain accuracy we use a second-order form Strang splitting and replace equation (A2) by

$$A(x + \xi, \cdot) \cong \exp(\xi D/2) \cdot \exp \left[\int_x^{x+\xi} G dx' \right] \cdot \exp(\xi D/2) (A(x, \cdot)) \quad (\text{A3})$$

The error in going from equations (A2) to (A3) is again a function of a commutator, $[D, G]$, and is proportional to ξ^3 . The advantage of this approximation is that numerical evaluation is straightforward for all terms on the right. The middle exponential is simply a function. The exponentials involving D are simple diffraction terms, and can be expressed using fast Fourier transforms (FFTs). Specifically

$$\exp(\xi D/2) A(x, \cdot) = \mathcal{F}^{-1} [e^{\xi v^2/2}] \mathcal{F}(A(x, \cdot)) \quad (\text{A4})$$

where \mathcal{F} is the Fourier transform with respect to z , v is the transform variable and \mathcal{F}^{-1} is the inverse transform. (The diffraction terms could instead be treated by, for example, a finite difference method.) A consequence of using Fourier transforms is that edge effects are avoided but replaced by periodicity in the vertical direction. This causes no difficulty, provided care is exercised in choosing the domain size.

Appendix B: Analysis of a single irregular feature

Focusing of a diverging field

We consider the conditions for producing amplification in the diverging field of a point source. The source is situated at the origin of the Cartesian system of axes (x, z) . A phase modulating feature given by

$$\exp\{-(\beta^2 + i\alpha^2)z^2\} \quad (\text{B1})$$

lies in the $x = 0$ plane, where

$$\beta = 2/D. \quad (\text{B2})$$

This lens-like feature has a width D . The maximum phase change imposed by the feature is ϕ_0 , the difference between its phase at $z = 0$ and $z = D/2$, i.e.

$$\phi_0 = \alpha^2 D^2/4 \quad (\text{B3})$$

whence

$$\alpha^2 = 4\phi_0/D^2 \quad (\text{B4})$$

The field on the x plane beyond $x = 0$ is given by the integral using the parabolic form of the wave equation

$$E(x, z) = \frac{E_0}{\sqrt{x_0(x-x_0)}} \times \int_{-\infty}^{\infty} \exp\{-(\beta^2 + i\alpha^2)z'^2\} \exp\left[\frac{ikz'^2}{2x_0} + \frac{ik(z-z'^2)}{2(x-x_0)}\right] dz' \quad (\text{B5})$$

Here the first term in the exponent is the phase-changing feature, the second is the field from the point over the x_0 plane, while the third term is the field over the x plane owing to a point (z', x_0) of the field just after the x_0 plane. We note that the second term represents a diverging field (from the point source). The imaginary part of the first term represents a converging field. For field amplification, or focusing, the converging term must be greater than the diverging one, i.e. it is required that

$$\alpha^2 > k/2x_0 \quad (\text{B6})$$

or, from equation (B3)

$$\phi_0 > kD^2/8x_0. \quad (\text{B7})$$

Equation (B5) can be easily evaluated and the field on the x axis found by setting z to zero. The intensity on the axis is then

$$I(0, x) = \frac{\pi E_0^2}{x_0(x-x_0)} \left[\beta^4 + \left(\alpha^2 - \frac{k}{2} \left[\frac{1}{x_0} + \frac{1}{x-x_0} \right] \right)^2 \right]^{-1/2} \quad (\text{B8})$$

The term outside the square brackets is the intensity decrease caused by circular spreading from the point source. The term in the square brackets is the effect of the lens-like feature relative to the circularly expanding field. The condition for it to be a maximum, i.e. for it to produce a focus, is

$$\alpha^2 = \frac{k}{2} \left[\frac{1}{x_0} + \frac{1}{x-x_0} \right] \quad (\text{B9})$$

This occurs at a distance $x = x_{\max}$

$$x_{\max} = x_0 \left[1 - \frac{k}{2\alpha^2 x_0} \right]^{-1} \quad (\text{B10})$$

Thus the condition for x_{\max} to be positive is

$$2\alpha^2 x_0/k > 1 \quad (\text{B11})$$

which is just equation (B6). In terms of the phase change imposed by the lens-like feature given in equation (B4) this requires that

$$\phi_0 > kD^2/8x_0. \quad (\text{B12})$$

As ϕ_0 increases beyond this critical value the position of the focus x_{\max} draws closer to x_0 equation (B9). Eventually for a close approach of the focus this relationship can be rewritten as

$$x_{\max} - x_0 = kD^2/8\phi_0. \quad (\text{B13})$$

Appendix C: Correlation between phase excursion and curvature

Correlation between wavefront phase and curvature

The cumulative phase modulation imposed on the wavefront by successive screens is

$$f(x, z) = \sum_i \phi_i(z) \quad (\text{C1})$$

where ϕ_i is the phase change in the i th screen at distance x' . The screens are statistically independent and so $f(x, z)$ is a Gaussian random process. It can be represented as

$$f(x, z) = \sum_v A(v) \cos(vz + \epsilon(v)) \quad (\text{C2})$$

The $\epsilon(v)$ are statistically independent and uniformly distributed between $\pm\pi$. The spatial frequency spectrum of the process $A(v)$ is the same as that of the individual screens.

The phase curvature of the modulated wavefront is its second derivative with respect to z

$$f''(x, z) = - \sum_v A(v)v^2 \cos(vz + \epsilon(v)) \quad (\text{C3})$$

while the cross-correlation between the phase modulation and its curvature is

$$\langle f(x, z_1)f(x, z_2) \rangle = - \sum_v A^2(v)v^2 \cos(v[z_1 - z_2]) \quad (\text{C4})$$

Passing to continuous notation this cross-correlation becomes

$$\rho_x(\zeta) = - \int A^2(v)v^2 \cos(v\zeta)dv, \quad (\text{C5})$$

the autocorrelation of the process $f(x, z)$ is

$$\rho(\zeta) = \int A^2(v) \cos(v\zeta)dv, \quad (\text{C6})$$

while

$$\rho_x(\zeta) = \partial^2 \rho(\zeta) / \partial \zeta^2. \quad (\text{C7})$$

Example

For a process f with a Gaussian autocorrelation function and scale size L

$$\rho(\zeta) = \exp\{-\zeta^2/L^2\} \quad (\text{C8})$$

while

$$\rho_x(\zeta) = -\frac{2}{L^2} \left(1 - 2\frac{\zeta^2}{L^2}\right) \exp\{-\zeta^2/L^2\} \quad (\text{C9})$$

This cross-correlation has a maximum (negative) correlation between the magnitude of the phase and its curvature at the same location.

Appendix D: Scattering angle and longitudinal extension of features

Scattering angle and longitudinal extension of features

The angular spectrum of the multiply scattered field from a point source in a random medium is

$$A(S) = \frac{1}{2\pi} \int C(\zeta) \exp(-ikS\zeta) d\zeta \quad (D1)$$

where S is the sine of the angle of the wave normal relative to the x axis and

$$C(\zeta) = \exp\left(-\beta x \left[1 - \int_0^1 R_0(\zeta s) ds\right]\right) \quad (D2)$$

is the autocorrelation of complex amplitude of the multiply scattered field ([11] p. 31). Here

$$R_0(\zeta) = R(\zeta)/R(0) \quad (D3)$$

is the normalized projected autocorrelation function of equation (6). Since we are interested in cases where βx is greater than unity, C is appreciable only for $R_0(\zeta)$ close to unity. Thus $R_0(\zeta)$ can be expanded in a Taylor series and only the first two terms kept. This gives finally

$$A(S) = (\sqrt{\pi} k S_0)^{-1} \exp\{-S^2/S_0^2\} \quad (D4)$$

where

$$S_0 = 2 \left(\frac{1}{3} \beta x R_0''(0) \right)^{1/2} / kL \quad (D5)$$

and we note that the second derivative of an autocorrelation function at the origin is negative. The wavelength of the radiation is much less than the scale size L , so we have that $kL \gg 1$. Thus $S_0 \ll 1$ since R_0'' is of order unity and βx is not very large unless we go to the very far field, well beyond the focus, in the weakly scattering medium that we are considering.

Acknowledgements

BJU was supported by the US Office of Naval Research, Award No. N00014-04-1-0472. MS acknowledges support from a UK DTI eScience grant and the resources of the Cambridge–Cranfield High-Performance Computing Facility.

References

- [1] Jakeman, E., 1988, Enhanced backscattering through a deep random phase screen. *Journal of Optical Society of America*, **5**, 1638–1648.
- [2] Ishimaru, A., 1978, *Wave Propagation and Scattering in Random Media* (New York: Academic Press).
- [3] Flatté, S. M., 1979, *Sound Transmission through a Fluctuating Ocean* (Cambridge: Cambridge University Press).
- [4] Uscinski, B. J., 1985, Range and time dependence of acoustic intensity fluctuations, *Ocean Seismo-acoustics NATO Conference Series IV; Marine Sciences*, **16**, 253–267 (New York: London Plenum Press).
- [5] Uscinski, B. J., 1989, Numerical simulations and moments of the field from a point source in a random medium. *Journal of Modern Optics*, **36**, 1631–1643.
- [6] Potter, J. R., Uscinski, B. J. and Akal, T., 2000, Random focusing of sound into spatially coherent regions. *Waves in Random and Conference Media*, **13**, 107–123.
- [7] Rytov, S. M., Kravtsov, Yu A. and Tatarskii, V. I., 1989, *Principles of Statistical Radiophysics* Vol. 4 (Berlin, Springer).

- [8] Codona, J. L., Creamer, D. B., Flatté, S. M., Frehlich, R. G. and Henyey, F. S., 1986, Solution for the fourth moment of waves propagating in random media. *Radio Science*, **21**, 929–948.
- [9] <http://www.damtp.cam.ac.uk/user/ms100/randommov.gif>.
- [10] <http://www.damtp.cam.ac.uk/user/ms100/angle.mpg>
- [11] Uscinski, B. J., 1977, *The Elements of Wave Propagation in Random Media* (New York, London: McGraw-Hill).
- [12] Keller, J. B. and Papadakis, J. S., 1977, *Wave Propagation and Underwater Acoustics* (Berlin: Springer).
- [13] Tappert, F. D. and Hardin, R. H., 1974, *Proceedings of 8th International Congress on Acoustics* Vol. II (London: Goldcrest).
- [14] Macaskill C. and Ewart T. E., 1984, Computer simulation of two-dimensional random wave propagation. *IMA Journal of Applied Mathematics*, **33**, 1–15.
- [15] Spivack, M., 1990, Operator splitting for the random wave moment equations. *Applied Mathematics Letters*, **3**, 87–91.